Quantitative proteomics reveals direct and indirect alterations in the histone code following methyltransferase knockdown†‡

Mariana D. Plazas-Mayorca,[a] Joshua S. Bloom,[bc] Ulrike Zeissler,[d] Gary Leroy,[b] Nicolas L. Young,[b] Peter A. DiMaggio,[b] Leonid Krugylak,[bcef] Robert Schneider[d] and Benjamin A. Garcia*[ab]

Histones are highly conserved proteins that organize cellular DNA. These proteins, especially their N-terminal domains, are adorned with many post-translational modifications (PTMs) such as lysine methylation, which are associated with active or repressed transcriptional states. The lysine methyltransferase G9a and its interaction partner Glp1 can mono- or dimethylate histone H3 on lysine (H3K9me1 or me2); possible cross-talk between these modifications and other PTMs on the same or other histone molecules is currently uncharacterized. In this study, we comprehensively analyze the effects of G9a/Glp1 knockdown on the most abundant histone modifications through both Bottom Up and Middle Down mass spectrometry-based proteomics. In addition to the expected decrease in H3K9me1/me2 we find that other degrees of methylation on K9 are affected by the reduction of G9a/Glp1 activity, particularly when K9 methylation occurs in combination with K14 acetylation. In line with this, an increase in K14 acetylation upon G9a knockdown was observed across all H3 variants (H3.1, H3.2 and H3.3), hinting at the potential existence of a binary switch between K9 methylation and K14 acetylation. Interestingly, we also detect changes in the abundance of other modifications (such as H3K79me2) in response to lowered levels of G9a/Glp1 suggesting histone PTM cross-talk amongst the H3 variants. In contrast, we find that G9a/Glp1 knockdown produces little effect on the levels of histone H4 PTMs, indicating low to no *trans*-histone PTM crosstalk. Lastly, we determined gene expression profiles of control and G9a/Glp1 knockdown cells, and we find that the G9a/Glp1 knockdown influences several genes, including DNA binding proteins and key factors in chromatin. Our results provide new insights into the intra- and inter- histone cross-regulation of histone K9 methylation and its potential downstream gene targets.

Introduction

Histones are basic proteins that package eukaryotic DNA into chromosomes. One-hundred and forty six base pairs of DNA wrap around an octameric histone core composed of two units each of histone variants H2A, H2B, H3 and H4.[1] Histone proteins, especially their N-terminal domains, are adorned with many post-translational modifications (PTMs) that occur in multiple but specific residues. These modifications have been proposed to act as a "code" which regulates gene expression by recruiting effector proteins with specialized binding domains leading to altered transcriptional states.[2] Altered chromatin structure—*via* histone modification—has been associated with many important cellular events including apoptosis,[3] cellular differentiation,[4] cancer,[5] and cell cycle progression.[1] Lysine acetylation and methylation are among the most prevalent histone modifications. Histone acetylation is usually correlated with transcriptional activation and has been proposed to affect the physical structure of chromatin through neutralization of the histone–DNA charge interaction[7] or by recruiting bromodomain-containing nucleosome remodeling complexes.[8] On the other hand, histone methylation can either signal for transcriptional activation or repression depending on the specific site of modification and its context.[8,9] For example, histone H3 tri-methylation at lysine 4 (H3K4me3) and lysine 36 (H3K36me3) are linked to promoter and transcribed regions and are correspondingly recognized by proteins containing Tudor and PHD domains.[7] Conversely, methylation of histone H3 on lysine 9 (H3K9me3) and lysine 27 (H3K27me3) are associated with repressed chromatin as these marks recruit the gene silencing proteins Heterochromatin Protein 1 (HP1) and Polycomb group (PcG), respectively.[8,10]

Depending on the particular histone variant and the specific site methylated, distinct enzymatic "writers" are responsible

[a] Department of Chemistry, Princeton University, Princeton, NJ 08540, USA. E-mail: bagarcia@princeton.edu; Fax: +1 609-258-1035; Tel: +1 609-258-8854
[b] Department of Molecular Biology, Princeton University, Princeton, NJ 08540, USA
[c] Lewis-Sigler Institute for Integrative Genomics, Princeton University, Princeton, NJ 08540, USA
[d] MPI for Immunobiology, Stübeweg 51, 79108 Freiburg, Germany
[e] Department of Ecology and Evolutionary Biology, Princeton University, Princeton, NJ 08540, USA
[f] Howard Hughes Medical Institute, Princeton University, Princeton, NJ 08540, USA

for adding different degrees of methylation. For instance, there are at least seven lysine histone methyltransferases (HMTases) responsible for the methylation of lysine 9 on histone H3 only.[6] For example, SUV39H1 adds two methyl groups to monomethylated K9 (resulting in H3K9me3) and heterochromatin formation.[11] In human cells, H3K9me2 is an abundant PTM that has been shown to be catalyzed by G9a (a euchromatic HMTase) and the related G9a-like protein 1 (Glp1) that has been shown to interact with G9a.[11] Knockout of either of these HMTases has lethal consequences for embryonic cells after concurrent reduction of both H3K9me1 and H3K9me2 levels and gene induction. H3K9 methylation has major roles in transcriptional control. G9a is capable of repressing gene activity in euchromatic regions by inducing histone methylation at target promoters.[12] Furthermore, G9a is unique in its ability to recruit DNA methylating enzymes,[13] and this function is independent of G9a's HMTase activity.[14,15] Interestingly, knockdown of G9a and the consequent reduction of H3K9 methylation cause relocation of HP1 in the genome. Given these intricate processes, it is feasible for G9a to affect the modification state of other histone PTM sites (aside from H3K9) through direct or indirect interactions with other proteins or by affecting H3K9 levels (histone PTM cross-talk). Therefore, determining the full collection of histone PTM patterns affected by this HMTase might reveal functional associations or cross-talk between co-existing histone PTMs and other proteins, and potentially illuminate downstream and upstream mechanisms directed by G9a function.

Quantitative characterization of the full effect of G9a (or any histone modifying enzyme) on histone PTM patterns has been difficult because most analyses of histone PTMs are achieved using qualitative measurements. Histone modifications have conventionally been analyzed through experiments involving modification-specific antibodies in immunoassay methods (such as Western blotting and immunofluorescence). Although these methods have provided a great deal of information about the association between histone PTMs and cellular processes, they are unable to detect and quantify multiple PTMs per histone molecule or novel PTMs. Furthermore, antibodies are susceptible to cross-reacting with other sites on the same or different protein, variable specificity, and epitope occlusion through interference by neighboring modifications within the recognized sequence.[16] Due to all these reasons, mass spectrometry (MS) has emerged as an alternative method to study histone modifications in a much more quantitative manner.[16] Analysis of histones by MS can be performed in several ways. For Bottom Up MS, histones are enzymatically digested into short peptides prior to mass spectrometry;[16] this method is very useful for characterizing and quantifying histone modifications as well as discovering novel low level PTMs on histones. Bottom Up PTM quantification entails the transformation of endogenously unmodified or monomethylated lysine residues into propionyl amides through reaction with d_0- or d_{10}-propionic anhydride[16] followed by trypsin digestion. This produces Arg-C-like peptides, as cleavage occurs only after arginine residues. Then, a second derivatization with either d_0- or d_{10}-propionic anhydride incorporates a stable isotope-label mass shift on the newly formed free N-terminal amino groups. Relative changes on histone PTM

abundance between two samples can be directly detected in a single experiment analyzing a mixture of the samples because histone peptides from the d_0-propionyl and d_5-propionyl labeled samples will appear as peak doublets separated by a $+5$ Da mass shift.[16] On the other hand, Top Down and Middle Down MS analyze intact proteins or large histone polypeptides, respectively, including detecting PTMs spanning several modifiable residues. As mentioned earlier, the majority of the histone PTMs are located within their N-terminal tail (spanning ~36 residues). Thus, Middle Down MS preserves the connectivity between most of the histone modification sites and in this way enables the identification of combinatorial PTMs found on single histone forms.[17]

In this report, we use quantitative Bottom Up and Middle Down proteomics in combination with RNA inhibition knockdown of G9a and Glp1 to comprehensively analyze the effect of this HMTase on histone modifications. At first, we quantify the expected decrease in K9me2, the major target of G9a/Glp1 in vivo. However, we find that reduction of G9a/Glp1 levels also influences other histone PTMs. Generally, our data suggest a synergistic interplay between H3K9me2 and H3K14ac. Reduction of G9a/Glp1, histone H3 containing both K9me2 and K14ac simultaneously, is steeply decreased compared to histone H3 containing K9me2 alone. Furthermore, K14ac levels drastically increase upon G9a/Glp1 knockdown. We also find H3K79 and H3K36 methylation increase with decreases in K9 methylation. A closer look at the modification profiles resulting from G9a/Glp1 knockdown for the three H3 variants (H3.1, H3.2 and H3.3) reveals slightly different effects for each histone isoform. We did not observe any evidence for trans-histone crosstalk, as the changes on H3 PTMs did not however translate into changes in histone H4 PTMs or H2A/H2B variant expression levels. Additionally, to provide a genome-wide view of the gene expression patterns differentially regulated by G9a/Glp1 HMTase activity, we measured mRNA abundances from control and G9a/Glp1 knockdown cells. Here we find that G9a/Glp1 reduction is associated with a unique transcriptional response consisting of an enrichment for DNA binding proteins in the subset of differentially expressed genes. Our proteomic and genomic results thus provide new insights into the cross-regulation of histone K9 methylation by G9a/Glp1.

Results and discussion

As G9a and Glp1 substrate specificity and potential cross-talk effects have not been adequately quantitatively characterized to date, we aimed to explore the global consequences of G9a and Glp1 depletion on histone modifications. It is generally accepted that G9a/Glp1 dimethylates H3K9,[11] but some reports have also suggested that G9a/Glp1 is partially responsible for K9me1 and even other histone residues such as H3K27 methylation.[18,19] To resolve these discrepancies, we purified histones from control human HEK 293 cells and HEK 293 cells in which G9a and Glp1 were knocked down through RNA interference and analyzed these histone samples through both Bottom Up and Middle Down mass spectrometry approaches. RT-PCR of both enzymes after the knock-down normalized to β-actin showed that abundance levels of the

proteins were reduced to between ∼40–60% (Fig. S1, ESI†). As mentioned previously, analysis of histones by MS can be performed in several ways: Top Down, Middle Down and Bottom Up (Fig. S2†).[16] Top Down and Middle Down MS methods analyze the concurrent modifications of intact proteins or large histone polypeptides, respectively. On the other hand, the Bottom Up approach enzymatically digests histones into short peptides prior to MS analysis. While this eliminates the connectivity between co-existing modifications, Bottom Up methods allow for both the characterization and quantification of histone modifications. For Bottom Up studies, we exploited a widely utilized chemical derivatization procedure (propionic anhydride derivatization) to facilitate analysis.[20] This approach has the advantages of producing reproducible peptides from highly basic proteins, removing charge facilitating MS/MS analysis via collision-activated dissociation, and improves chromatographic retention characteristics of hydrophilic peptides. This method also allows for the use of both light (d_0) and heavy (d_{10}) propionic anhydride to isotopically label samples for relative quantification between the samples, analyzing all histones in a "one-pot" analysis.[21] We have previously shown that resulting histone peptides from two different samples can be directly compared through nanoLC-MS/MS analysis, and relative variations in histone PTM levels between samples can be accessed as histone peptides from the d_0-propionyl and d_5-propionyl labeled samples will appear as peak doublets separated by a +5 Da mass shift.[21] We used this type of post-protein isolation stable isotope labeling to detect differential expression of histone marks upon G9a and Glp1 knockdown as depicted in Fig. 1. For these investigations, we decided to interrogate the purified histone variants (H4, H3.1, H3.2 and H3.3) separately, as it has been previously suggested that the different H3 variants may be modified differently or may be acted upon differently by histone modifying enzymes.[22,23] To obtain purified histone variants, we fractionated out the histone variants from total acid extracts through reverse phase high performance liquid chromatography (RP-HPLC) as previously performed.[22] Histone proteins from the control and G9a/Glp1 knockdown HEK 293 cells were then derivatized with two rounds of d_0-propionic anhydride and digested with trypsin. Histone peptides from control HEK cells were labeled in the second derivatization with d_0-propionic anhydride, while histone peptides from the G9a/Glp1 knockdown cells were labeled in the second derivatization with d_{10}-propionic anhydride. These samples are equally mixed and then analyzed by MS. This introduces a d_5-propionyl amide group on the N-terminus of each peptide, resulting in a +5 Da shift. For doubly charged peptides, the original mass difference of +5 Da translates into a mass shift of +2.5 m/z between knockdown and control peptides and for triply charged peptides,
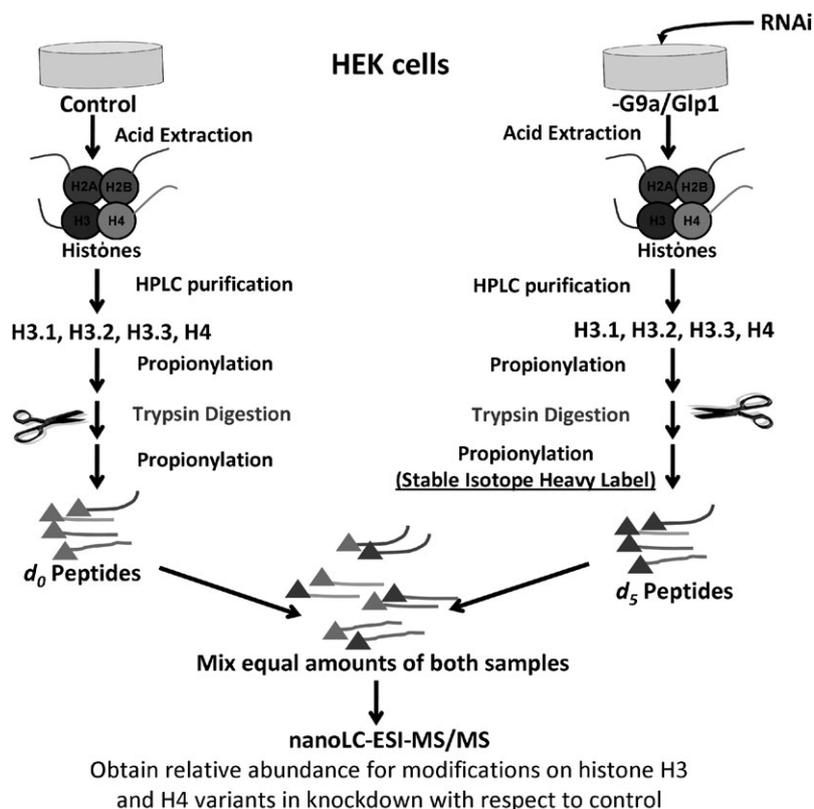
Fig. 1 Schematic description of histone PTM characterization after G9a/Glp1 knockdown through chemical derivatization and stable isotope peptide labeling for quantitative proteomics. Histones are acid extracted from control HEK and HEK cells previously treated with siRNA to produce a G9a/Glp1 knockdown by RNA interference. Histones from each sample are purified by HPLC, propionylated and then digested with trypsin. Resulting peptides are then subjected to a second round of propionylation. A stable isotope label is introduced in this step for one of the samples, as this allows for the relative quantification of histone H3 and H4 modifications between the samples.

there will be a $+1.66$ m/z mass shift difference. Reverse labeling (d_5 for control and d_0 for knockdown) was also performed and included in the results.

An example of our quantitative proteomic approach for investigating G9a/Glp1 activity is shown in Fig. 2. Here, we observe the effects of the G9a/Glp1 knockdown on a peptide spanning the 9–17 residues of histone H3.1 containing the K9 residue. We detect a set of peaks at 535.305 and 537.821 m/z, respectively, that correspond to the 9–17 peptide $_{pr}$-K$_{pr}$STGGK$_{pr}$APR (Fig. 2A). Accurate mass (<2 ppm error for both peptides) and MS/MS spectra (not shown) indicate these peptides being endogenously unmodified as evident by the conversion of the unmodified lysines to d_0 and d_5-propionyl amides (pr). We find that the unmodified K9 peptide is at least 2-fold higher in the G9a/Glp1 knockdown relative to the control. Conversely, we detect decreases in both K9me1 and K9me2 levels with decreasing G9a/Glp1 expression, with a more significant effect occurring on H3K9me2 (Fig. 2B and C). Generally, we detected no decrease in H3K9me3 levels in the G9a/Glp1 depleted cells (Fig. 2D). Our data are consistent with previous literature reporting that G9a/Glp1 are the main enzymes responsible for generating K9me2 in a single step through the addition of two methyl groups to unmodified H3K9.[11] Our results for H3.1 are also in agreement with prior reports indicating that G9a activity is linked with K9 mono-methylation to a much lesser degree.

In addition to K9 methylation, we also examined the effect of G9a/Glp1 knockdown on several other well known methylation sites on histone H3 such as K4, K27, K36 and K79. Fig. 3 shows the results of our quantitative proteomics on histone H3.2 peptides spanning regions containing K4 (Fig. 3A), K27 (Fig. 3B), K36 (Fig. 3C) and K79 (Fig. 3D)

dimethylation. G9a/Glp1 depletion has no discernable effect on K4me2 (Fig. 3A), with modest influences on K27 or K36 dimethylation (Fig. 3B and C). Interestingly, opposite effects were detected on these methylation sites, as K27me2 slightly decreases and K36me2 slightly increases upon G9a/Glp1 knockdown (Fig. 3B and C). Surprisingly, we did observe a large change in K79 dimethylation: K79me2 was approximately 2-fold higher in the knockdown cells compared to control (Fig. 3D). Lysine 79 is methylated by the HMTase DOT1,[24] and unlike K27 or K36 is found on the core histone fold region of H3. Given that K9 dimethylation has been correlated with transcriptional silencing and H3K79 methylation has been correlated with active genes,[25,26] our results seem to suggest tandem inverse regulation of these modifications. The smaller changes detected on K27 and K36 dimethylation also support this hypothesis.

For relative quantification of histone modifications, the abundance level of each modified peptide was estimated by measuring the abundance (single ion chromatogram) of the modified peptide and expressing that as the ratio of the modified peptide over the sum of the modified and unmodified forms of that peptide, as previously performed for histone PTM analysis.[22,27] For comparison of the histone marks between control and G9a/Glp1 knockdown samples, the relative abundance of a particular histone mark in the control sample was divided by the abundance of the same mark in the G9a/Glp1 knockdown cells to obtain a fold-enrichment ratio. Such ratios were plotted in a heat map, with red and green, respectively, indicating an increase or decrease for that mark in the G9a/Glp1 knockdown cells for histones H3.1, H3.2 and H3.3 (Fig. 4 and Fig. S3, ESI†). Our results show that most of the histone H3 marks do not exhibit changes greater than
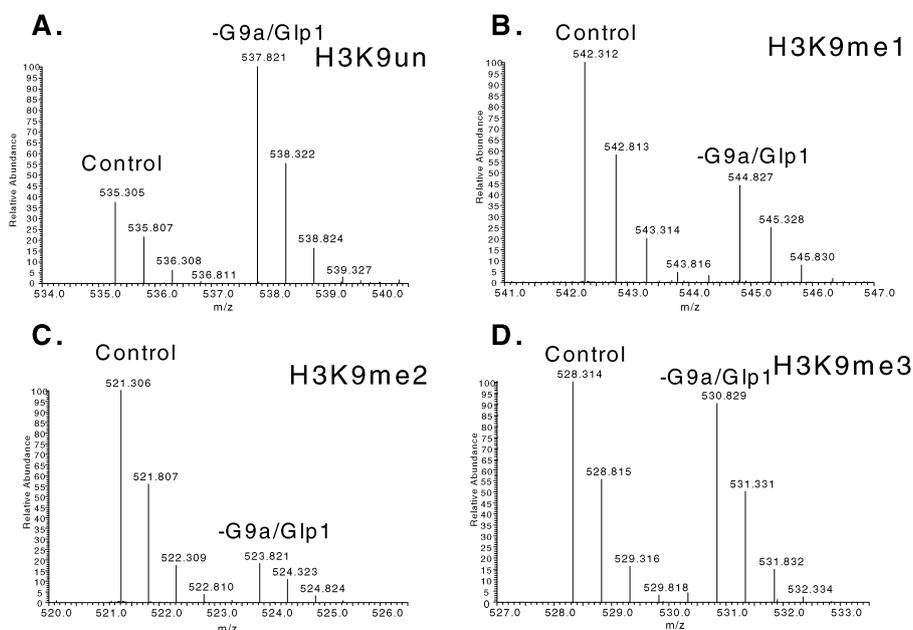
Fig. 2 Comparison of histone H3.1 K9 modified peptides from control cells (d_0-labeled) and cells with G9a/Glp1 knockdown (d_5-labeled) following quantitative Bottom Up MS. A. Full mass spectrum for the 2+ charge state of the unmodified H3K9 peptide (9–17 residues). B. Full mass spectrum for the 2+ charge state of H3K9me1 peptide (9–17 residues). C. Full mass spectrum for the 2+ charge state of the H3K9me2 peptide (9–17 residues). D. Full mass spectrum for the 2+ charge state of H3K9me3 peptide (9–17 residues).
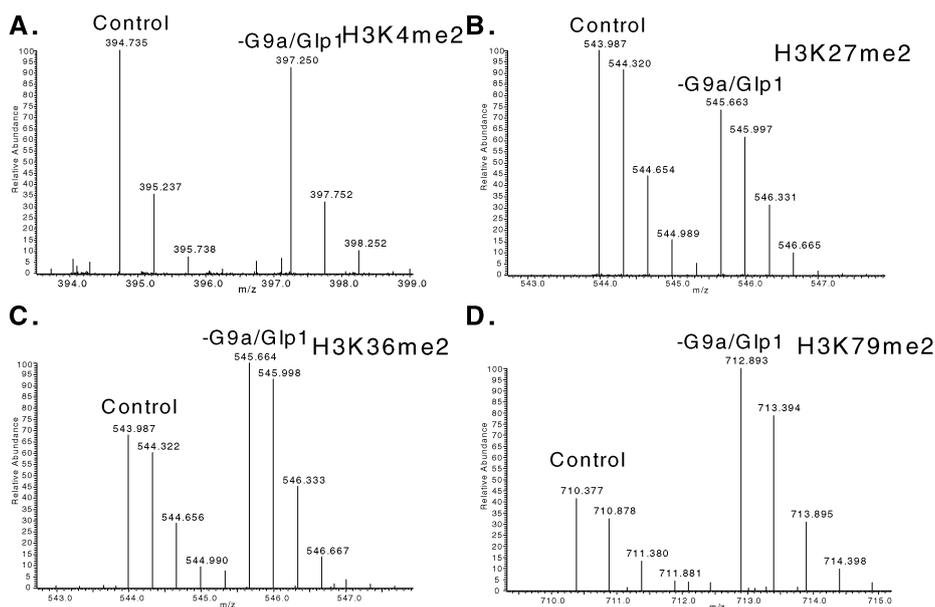
Fig. 3 Comparison of other non-K9 methylated histone H3.2 peptides from control cells (d_0-labeled) and cells with siRNA G9a/Glp1 knockdown (d_5-labeled) following quantitative Bottom Up MS. A. Full mass spectrum for the 2+ charge state of the unmodified H3K4me2 peptide (9–17 residues). B. Full mass spectrum for the 2+ charge state of H3K27me2 peptide (9–17 residues). C. Full mass spectrum for the 2+ charge state of the H3K36me2 peptide (9–17 residues). D. Full mass spectrum for the 2+ charge state of H3K79me2 peptide (9–17 residues).
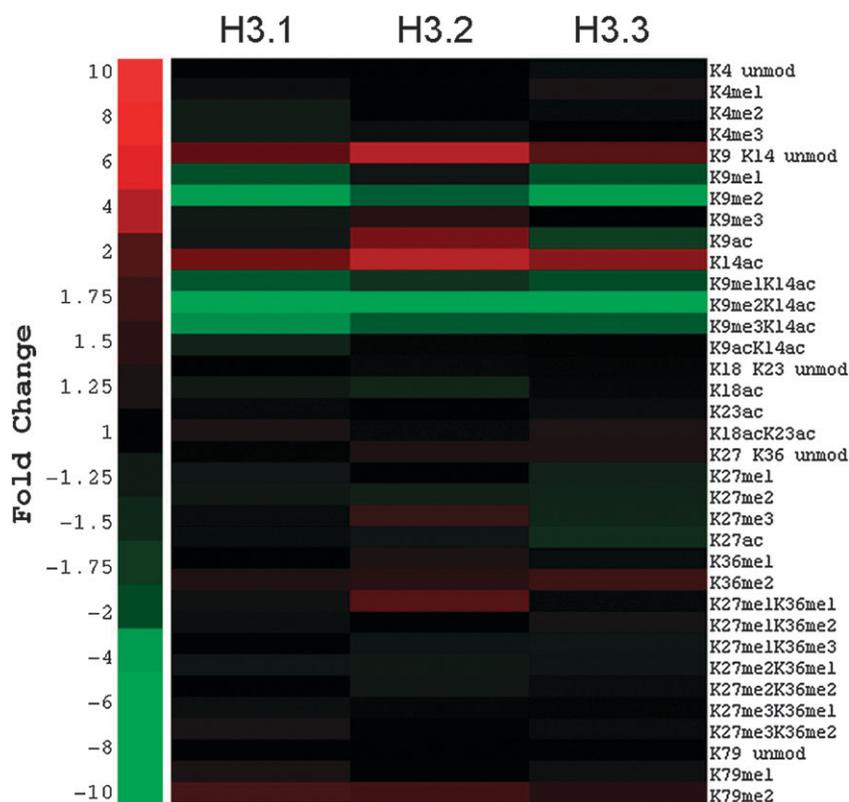

Fig. 4 Heatmap depicting the ratio of histone H3 PTM abundances in G9a/Glp1 knockdown cells relative to control cells for histone variants H3.1, H3.2 and H3.3. The scale indicates the fold change between a given PTM abundance in the G9a/Glp1 knockdown *versus* control. Red and green indicate an increase or decrease in the abundance of a given PTM in cells with lowered G9a/Glp1 levels.

1.5 fold (Fig. 4). Nevertheless, the modification sites that have the largest fold changes upon G9a/Glp1 knockdown are consistent regardless which histone H3 variant they reside on. For example, K9me2 levels decrease throughout all variants, but larger fold changes occur in the H3.1 and H3.3 variants

(4-fold change) in comparison to H3.2 (2-fold change). K9 unmodified levels increase for all the H3 variants, again with slightly different levels seen on H3.2 compared to the other two variants. Reproducible changes on K27, K36 and K79 are also observed for all variants. In contrast, K9 monomethylation decreases on histones H3.1 and H3.3, but it does not on histone H3.2. All degrees of methylation on K27 decrease on the H3.3 variant in the knockdown cells, but do not change on H3.1. Interestingly, for the H3.2 variant, K9me3 reproducibly show a very modest increase in the G9a/Glp1 RNAi treated cells. This is particularly interesting as most H3K9 methyl-transferases convert K9 from the me1 to me3 state, except ASH1 (converts unmodified K9 to me3).[28] These H3 variant-dependent PTM level differences in the G9a/Glp1 knockdown cells may also be a result of the genomic location of the H3 variants, which has been suggested to be different, at least largely for the H3.3 variant. G9a is known to be enriched in silent euchromatin,[29] and the similar changes occurring on H3.1 and H3.3 compared to H3.2 seem to suggest that G9a may be endogenously located in genomic regions (*i.e.* euchromatic genes) where H3.3 and H3.1 may possibly co-reside. The H3.3 variant is known to be deposited independent of the cell cycle on active genes in several organisms,[23,30] however, less is known about the genomic residence of H3.1. Other reports in human and drosophila cells also suggest that H3.2 may be more heterochromatic in nature,[22,27] and thus our results showing different or less dramatic PTM changes on H3.2 compared to H3.1 or H3.3 would also be consistent with G9a being found in euchromatic regions of the genome, where H3.2 may be less abundant.

Through our Bottom Up MS experiments we can readily characterize many acetylation sites on H3 at K9, K14, K18, K23 and K27. After quantification of the histone acetylation sites, we found no appreciable differences in the acetylation levels on K18, K23 or K27 (Fig. 4). Still, as we quantified a peptide corresponding to the 9–17 fragment with a monoacetyl addition, we determined that this specific peptide was greatly increased in the G9a/Glp1 RNAi treated sample (Fig. 5A). At first, we speculated that this modified peptide must be H3K9ac, since we anticipated an increase in this mark as knockdown of G9a/Glp1 produces more K9 unmodified substrate that could be then acetylated by the appropriate histone acetyltransferase (HAT). However, peptides containing H3K9ac or H3K14ac often co-elute under our nanoflowLC conditions. To calculate exactly how much contribution H3K9ac or H3K14ac is making to the monoacetyl parent ion peak we must inspect the fragment ions in the MS/MS spectrum, and quantify them using a fragment ion relative ratio approach.[31] From the MS/MS spectrum, we can precisely determine the fraction of either K9ac or K14ac by inspection of several ions. In particular, we can use the b_1 ion, as when K14 is acetylated then K9 will be unmodified and this b_1 ion corresponding to K9un will have a mass of 241 Da (Lys residue 128 Da, 2 propionyl amide groups on the N-terminus and side chain of Lys, 112 Da, and 1 proton). On the other hand, if K9 is acetylated, then the mass of the b_1 ion will be 227 Da (Lys residue 128 Da, 1 propionyl amide group on the N-terminus, 56 Da, one acetyl group on the side chain of Lys, 42 Da, and 1 proton). Fig. 5B shows the MS/MS spectrum of
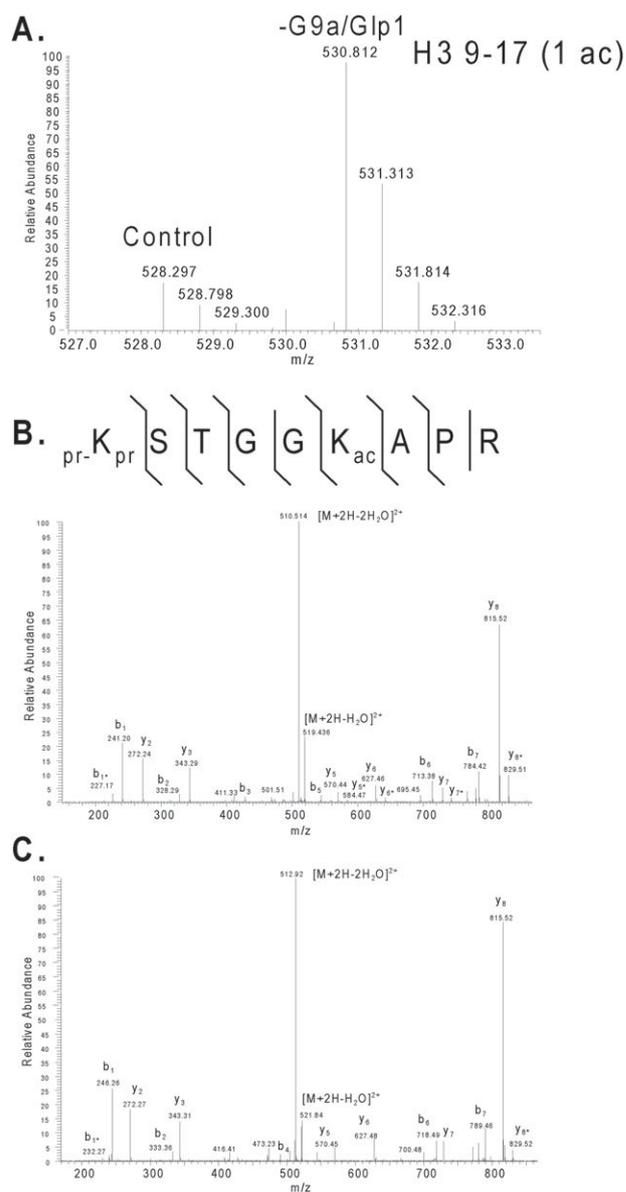
Fig. 5 Characterization of the differentially expressed monoacetyl peptide found to be increased in the G9a/Glp1 knockdown samples. A. Full mass spectrum of the $[M + 2H]^{2+}$ precursor ions spanning the 527–533 m/z region showing peaks at 528.297 m/z from control cells (d_0-labeled) and 530.812 m/z from cells with G9a/Glp1 knockdown (d_5-labeled). B. Averaged composite MS/MS spectrum of the precursor ion at 528.297 m/z (control, d_0 labeled), which upon manual inspection was found to be a mixture of both K9ac (227 Da fragment ion) and K14ac (241 Da fragment ion), with K14ac being most abundant on the peptide KSTGGKAPR. C. Averaged composite MS/MS spectrum of the precursor ion at 530.813 m/z (G9a/Glp1 knockdown, d_5 labeled), which upon manual inspection was found to be a mixture of both K9ac (232 Da fragment ion) and K14ac (246 Da fragment ion), with again K14ac being the most abundant species. Ions indicative of K9 acetylation are labeled with an asterisk in both spectra.

the precursor ion at 528.297 m/z from the control sample shown in Fig. 5A. Examination of the low m/z range demonstrates that the ion at 241 Da is nearly ten times higher in abundance than the ion at 227 Da. This indicates that the

monoacetyl peptide at 528.297 m/z is mostly composed of H3K14ac. Other ions denoted with an asterisk also report the same outcome that H3K14ac is the main species present in this multiplexed MS/MS spectrum. The MS/MS spectrum (Fig. 5C) from the same monoacetyl peptide from the G9a/Glp1 knockdown cells (530.812 m/z) shows the same result. This time the reporter ions indicative of K9 or K14 acetylation are shifted by 5 Da due to the d_5-propionyl label used on the N-terminus (232 and 246 Da). Again, the signal from the K14ac species (246 Da) dominates over the K9ac species (232 Da). Our results point to a discernable increase in K14ac upon G9a/Glp1 inhibition across all H3 variants (Fig. 4). Unexpectedly, K9 acetylation levels remain nearly constant in the H3.1 and H3.3 variants and only increase in the H3.2 variant, but not to the level of increase that is seen for K14.

Mounting experimental evidence strongly suggests that coexisting histone PTMs act in concert to govern gene expression.[32,33] Cross-talk has been convincingly shown to occur between K4 methylation and K14 acetylation in both human and yeast.[34,35] These short-range histone PTM combinations could reveal possible intra-histone modification cross-talk involving K9me2 afforded by G9a/Glp1 activity. Our Bottom Up analyses only allowed us to monitor peptides containing combinatorial K9 and K14, K18 and K23, or K27 and K36 modifications together. From the data depicted in Fig. 4, we observe that all methylation states on K9 are markedly decreased for all histone variants when the methylation occurs simultaneously with K14 acetylation. The decrease on this dually modified peptide is more prominent than the decrease on K9 methylation alone (Fig. 4 and Fig. S3, ESI†). This may result from G9a being found on euchromatin where the H3K9me2K14ac are found in higher abundance than H3K9me2 alone. Indeed, the H3K9me2 mark has been linked to more heterochromatic regions.[36] We now detect that H3K9me3K14ac levels decrease reproducibly across all H3 variants. Interestingly, H3K9me3 levels alone do not decrease reproducibly (Fig. 4). Binding of protein readers to particular histone PTMs might be influenced by other histone PTMs. For instance, regulation of heterochromatin protein 1 binding to H3K9me3 is provided by phosphorylation of serine 10 (the adjacent residue to lysine 9), and phosphorylation of this residue releases HP1 from chromatin.[32] This effect is known as the "Binary Switch".[37,38] Our data suggest that another possible binary switch may be present between K9 and K14. We envision a scenario in which K9 methylation either directly or indirectly hinders K14 acetylation, such that when K9 methylation is present, K14 is much less acetylated than when K9 is unmodified and also vice versa. This hypothesis would be consistent with the increase in the K14ac histone form observed in the G9a/Glp1 knockdown (Fig. 4 and 5).

As short range histone PTM combinations generally did not seem to be affected by G9a/Glp1 RNAi reduction, we decided to use a Middle Down proteomic method we previously utilized for monitoring long range combinatorial PTMs spanning the first 50 residues of histone H3.[39] This technique is based on combining on-line nanoflow hydrophilic interaction chromatography (HILIC) with electron transfer dissociation (ETD) based sequencing of the 1–50 amino acid histone H3 polypeptide followed by computational analysis using a mixed

integer linear optimization approach to solve the combinatorial modification superposition problem resulting from sequencing multiple modified forms.[39,40] This approach has allowed us to identify and quantify hundreds of combinatorially modified histone H3 forms in a single high-throughput experiment, with unprecedented speed, accuracy and precise measurement. Fig. 6A displays heatmap plots of the combinatorially modified forms generated after subjecting histone H3.1 from control and G9a/Glp1 depleted cells to this Middle Down MS analysis. The heatmap shows that although there is extensive overlap in forms detected between the samples, there are also some dramatic changes in the types of combinatorial forms differentially expressed between samples (Fig. 6A). There is a large increase in the number and abundance of unacetylated H3.1 1–50 forms from control to G9a/Glp1 knockdown. This is most likely a result of decreasing the amount of H3K9me2 forms and also decreasing the H3 methylated forms that are found in combination with K14ac, in agreement with our Bottom Up MS data. The majority of the forms changing in abundance contain both K9me2 and K14ac, as shown in the tandem mass spectrum of the form H3.1K9me2K14acK27me2K36me2 shown in Fig. 6B. No other correlations with other combinatorial PTM patterns were found.

Some histone modifications have been shown to be cross-regulated by the presence or absence of other modifications—on a different histone (usually within the same nucleosome).[41] For example, H3 K36 di- and trimethylation by the HMTase
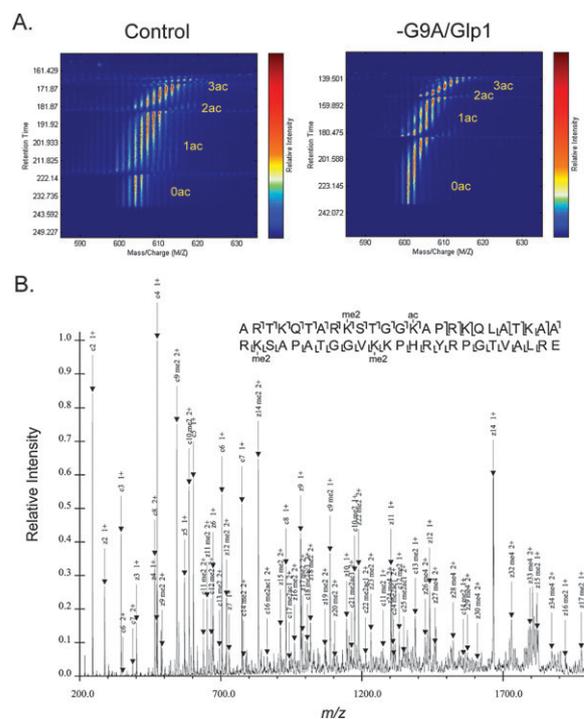
Fig. 6 Middle Down mass spectrometry characterization of long range combinatorially modified histone H3.1 forms. A. Heatmaps displaying the combinatorially modified H3.1 forms from control (left) and G9a/Glp1 depleted cells (right). B. ETD MS/MS spectrum of one of the differentially expressed forms (circled in G9a/Glp1 knockdown heatmap in (A)) found decreasing in the G9a/Glp1 knockdown cells. This H3 form was identified as H3.1K9me2K14acK27me2K36me2.

SET2 is *trans*-regulated by a critical lysine residue on histone H4. Here, the N-terminus of SET2 needs to interact with a basic patch around H4K44 in order to be able to properly bind nucleosomes and methylate H3K36.[42] We used our stable isotope labeling approach to investigate histone crosstalk on histone H4 modifications in the G9a/Glp1 knockdown cells. Results from these experiments are presented in Fig. S4 (ESI†). Our proteomic approach allows us to detect several known histone H4 acetylation sites and methylation at K20, however, we find practically no effect on the H4 PTMs following knockdown of the methyltransferases G9a and Glp1. Only a slight increase in K20me1 was detected upon G9a/Glp1 knockdown, suggesting that G9a/Glp1 activity produces little *trans*-histone cross-talk on histone H4. Additionally, we also monitored the post-translational modification levels of histone H2A and H2B variants on a combined total of 12 variants. As for histone H4, we did not observe any changes in the expression levels of any PTMs following G9a/Glp1 depletion (data not shown).

Finally, we ascertained the effects of G9a/Glp1 knockdown on gene expression patterns in the HEK cells using DNA microarrays. Biological replicates were highly correlated, Pearson $R = 0.88$, $p < 2.2 \times 10^{-16}$ and out of the 37 365 transcripts with high-quality data, 5201 were differentially expressed (Fig. 7, FDR < 5%). Genes up-regulated after knockdown of G9a/Glp1 were enriched for multiple gene ontology (GO) terms (FDR < 5%) that spanned several areas of biological function. Most notably, several genes were classified as DNA binding proteins; these were as diverse as transcription factors, to known components of chromatin remodeling complexes and histone modifying enzymes. Some of the histone modifying enzymes affected upon knockdown of G9a/Glp1 included MLL3 (2.12 fold) and ASH1 (1.40 fold), which are both upregulated. MLL3 and ASH1 are both histone HMTases that modify histone H3K4,[11] and thus may act opposite to G9a/Glp1 in function. Interestingly, we only observed a small, but reproducible increase in H3.1

K4me3 amongst the H3 variants. ASH1 has been also suggested to possess H3K9me3 activity;[11] consistently, we did observe a small increase in H3K9me3 levels on the H3.2 variant. Expression levels of EZH2 (0.73 fold), the K27 methyltransferase, were reduced upon G9a/Glp1 knockdown, consistent with our observed slight decrease in expression of this modification. However, we did not detect a change in the expression level of DOT1 (1.1 fold), the H3K79 HMTase, although we determined that H3K79 methylation decreases in the knockdown. Thus, the knockdown of G9a/Glp1 may affect DOT1 activity, but not its expression. We also observed changes in gene expression of other chromatin-associated proteins that are known to interact with different histone modifying enzymes. For example, SMAD1 (1.7 fold) has been shown to interact with the gene repressive HDAC/Sin3A complex in an Nkx3.2 and SMAD4 dependent manner.[43] Additionally, we also detected an increase of the protein cAMP-response element modulator (CREM), which has recently been found to be recruited to chromatin and whose gene expression is in part regulated by the demethylase Jmjd1a, the target of which is H3K9me1 and me2 in spermatocytes.[44] Lowered H3K9me2 levels in cells with decreased G9a/Glp1 may allow for upregulation of CREM in the absence of Jmjd1a activity. Lastly, we found that the expression of a number of histone genes were altered in response to G9a/Glp1 knockdown including members of all histone families. The significance of these changes remains to be determined.

Conclusions

We comprehensively characterize the effects of G9a/Glp1 knockdown on histone modification patterns using quantitative stable isotope labeling in combination with Bottom Up as well as Middle Down mass spectrometry-based proteomics. In addition to the expected decrease in K9me2, we find that mono and tri-methylation of K9 are also decreased upon reduction of G9a/Glp1 levels, in particular when K9 methylation occurs simultaneously with K14 acetylation. K14 acetylation occurring without K9 methylation also increases after G9a/Glp1 knockdown. These results suggest a possible short range combinatorial PTM binary switch between K9 and K14, the significance of which remains to be determined. In all, our findings suggest that removal of the HMTase G9a/Glp1 not only influences H3K9 dimethylation, but also some other histone H3 PTMs as well, such as dimethylation on the core residue K79. Methylation on this residue is increased in the absence of G9a/Glp1. We found histone H4 modifications are not affected by G9a/Glp1 knockdown, arguing against *trans*-histone cross-talk. Using a Middle Down mass spectrometry approach we interrogated possible long range combinatorial modifications on histone H3, and confirmed that long polypeptides containing both K9me2 and K14ac changed the most upon G9a/Glp1 knockdown. Finally, we assessed the effect of G9a/Glp1 knockdown on gene expression levels. This knockdown affects gene expression of several thousand genes spanning many types of biological functions, including several important factors involved in chromatin remodeling and transcription.
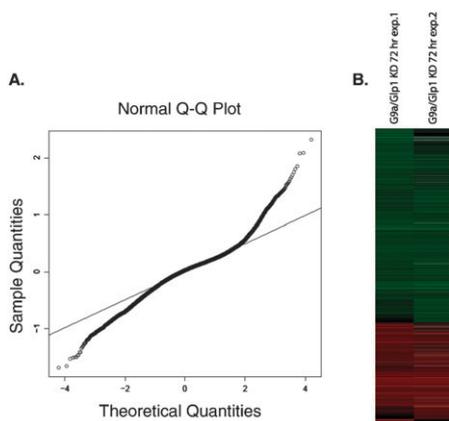
Fig. 7 A. Q–Q normal plot of 37 365 log$_2$ (G9a/Glp1 knockdown/reference) gene expression ratios. The majority of points lie within a normal distribution (line). The large positive and negative tails reflect the 1917 upregulated genes and 3284 downregulated genes at an FDR < 1%. B. Heatmap plot of the differentially expressed genes in the two G9a/Glp1 knockdown experiments.

Methods

Mammalian cell culture, nuclei isolation and histone extraction

4×10^6 HEK293 cells were plated in a 14.5 cm dish and grown under standard conditions. We then simultaneously transfected according to manufacturer's instructions with a mix containing 100 µl of 10 mM anti-Glp1 siRNA (AACGAAGAATGG-GAACCTATA, QIAGEN), 100 µl anti-G9a siRNA (CAC-CATGAACATCGATCGCAA, QIAGEN) and 100 µl of lipofectamine for double knockdown. Control cells were transfected with 200 µl 10 mM AllStars negative siRNA (QIAGEN). HEK293 cells are a standard cell line to perform knockdown experiments, and as such, we did not observe an immune response initiated by the transfection of the siRNA oligonucleotides. Nuclei were isolated and histone proteins were extracted after 48 h siRNA treatment as described by Garcia *et al.*[17] Briefly, histones were acid extracted from nuclei with 0.4 N H_2SO_4 and precipitated with trichloroacetic acid (TCA), followed by washes with acetone containing 0.1% HCl and then pure acetone. The resulting pellets were redissolved in deionized water prior to further processing. Total protein concentrations of each acid extract were determined using the Bradford assay.

RP-HPLC fractionation of bulk histones

Acid extracted bulk histones were separated as described by Garcia *et al.*[45] Briefly, acid extracts from nuclei were fractionated on a C18 column (4.6 mm id × 250 mm, Vydac, Hesperia, CA) using a Beckman Coulter System Gold HPLC (Fullerton, CA) with a gradient of 30–60% B in 100 min, followed by 60–100% B in 20 min (A = 5% MeCN in 0.2% TFA and B = 90% acetonitrile in 0.188% TFA). Fractions were collected in 1 min time intervals, pooled and dried to completion in a SpeedVac. An aliquot of the protein fractions were checked for quality using 15% SDS-PAGE.

Histone sample preparation for mass spectrometry

Bulk acid extracted histones (~ 50 µg) or HPLC purified histone variants (< 5 µg) were derivatized by treatment with propionyl anhydride reagent essentially as described before.[21,46] Briefly, this reagent was prepared using 75 µL of MeOH and 25 µL of propionic anhydride (Sigma Aldrich, St. Louis, MO). Equal volumes of reagent and histone protein were mixed and allowed to react at 37 °C for 15 min and reduced to near dryness using a SpeedVac concentrator for removal of reaction remnants. Propionylated histones were then digested with trypsin (Promega, Madison, WI) at a substrate/enzyme ratio of 20 : 1 for 6 h at 37 °C after dilution of the sample with 100 mM ammonium bicarbonate buffer solution (pH = 8.0). The reaction was quenched by the addition of concentrated acetic acid and freezing (-80 °C). A second round of propionyl-ation was then performed to propionylate the newly created peptide N-termini. For quantification studies, samples were stable isotope labeled using d_{10}-propionic anhydride (Cambridge Isotope Laboratories, Inc., Andover, MA).[21] For example, one sample was derivatized using d_0-propionic anhydride both before and after trypsin digestion, while a second sample was derivatized using d_0-propionic anhydride before trypsin digestion and derivatized with d_{10} reagent after trypsin digestion (introducing a $+5$ Da mass shift). For doubly and triply charged peptides, this mass difference translates into a 2.5 or 1.67 m/z shift respectively. For comparative MS analysis, protein concentrations of each sample were determined using Bradford assays and then samples were accordingly mixed for equal protein quantity.

Mass spectrometry

A small aliquot of the histone digests were desalted using in-house made C_{18} STAGE Tips prepared as previously described,[47] and loaded by an Eksigent AS-2 autosampler (Eksigent Technologies Inc., Dublin, CA) onto a fused silica microcapillary (75 µm) column constructed with an ESI tip and packed in-house with 5 µm C_{18} YMC ODS-A resin. Peptides were HPLC separated with an Agilent 1200 series binary pump with an in-line flow splitter across a 110 min linear gradient ranging from 2% to 35% buffer B (buffer A = 0.1 M acetic acid, buffer B = 70% acetonitrile in 0.1 M acetic acid) with a constant flow of approximately 200 nl min^{-1}. Additionally, Middle Down experiments on the 1–50 N-terminus of histone H3 were also performed as recently described.[39] In brief, histone H3 was digested with GluC and purified by HPLC as previously described to isolate the 1–50 amino acid H3 fragment. The modified forms were then separated using on-line nanoflowLC hydrophilic interaction chromatography with a gradient of 0–100% B in 250 min (solvent A = 75% acetonitrile, 20 mM propionic acid adjusted to pH 6.0 using ammonium hydroxide and solvent B = 25% acetonitrile adjusted to pH 2.5 with formic acid). The HPLC system was coupled to an LTQ-Orbitrap mass spectrometer (ThermoFisher Scientific, San Jose, CA) taking a full scan MS spectrum (m/z 290–1650) in the Orbitrap with a resolution of 30 000 after accumulation of approximately 500 000 ions followed by collisionally activated dissociation (CAD) of the seven most intense ions in the LTQ after accumulation of approximately 10 000 ions. All data were collected in centroid mode. Maximum filling time was 500 ms for the full scans. The decision-tree algorithm was used to perform concurrent CAD and electron transfer dissociation (ETD) fragmentation in the same experiment, deciding in real time which fragmentation method to employ based on the charge state and m/z of the precursor as previously described.[48] For ETD, an automatic gain control value of 3E6 for the reagent anion and a reaction time of 80 ms were used. Precursor ion charge state screening was enabled and all unassigned charge states as well as singly charged species were rejected. The dynamic exclusion list was restricted to a maximum of 500 entries with a maximum retention period of 120 s and a relative mass window of < 1 Da.

MS data analysis

CAD mass spectra were searched using the SEQUEST algorithm within the Bioworks Browser (Version 3.3.1 SP1, Thermo-Fisher Scientific Inc., San Jose, CA) against both human or yeast protein databases and human and yeast histone protein database derived from sequences obtained from the National

Center for Biotechnology Information (NCBI) database (August 2008). Trypsin protein sequence was also included in the databases. Enzyme specificity was set to trypsin, fully enzymatic, allowing for up to 3 missed cleavage sites (since endogenous and chemical modification of lysine residues hinders enzymatic digestion). Propionylation ($+56.026$ Da) on the N-terminus of the peptides was set as a fixed modification, while oxidation of methionine ($+15.995$ Da) was set as a variable modification for all searches. For histone PTM searches, propionylation ($+56.026$ Da), acetylation ($+42.010$ Da), mono- ($+70.042$ Da), di- ($+28.031$ Da) and trimethylation ($+42.046$ Da) of lysine residues were selected as variable modifications. Histone monomethylation was searched as the sum of the masses for propionylation ($+56.026$ Da) and methylation ($+14.016$ Da) because monomethylated residues can still be propionylated. Parent mass tolerance was set to 0.1 Da and fragment ion tolerance was set to 0.5 Da. Resulting peptide lists were filtered using standard criteria as previously used.[49] Additionally, we also used a peptide probability cutoff of 1×10^{-3} as calculated by the Bioworks program. The false discovery rate was estimated to be 1% for peptide IDs after searching reverse databases. All MS/MS spectra from modified peptides were also manually inspected for accurate mass and correct fragment assignment. Relative quantification of histone modifications was determined by measuring the area under the extracted ion chromatogram peak corresponding to a specific modified peptide normalized to the sum of the peak areas corresponding to all observed modified forms of such peptide. Fold change was calculated by taking the abundance of a given modification in the G9a knockdown and dividing it over the abundance of the same modification in control cells. A fold change higher than 1 would indicate an increase in the abundance of a given modification in the G9a knockdown, while a fold change lower than 1 would indicate a decrease in the modification abundance when G9a is knocked down. Heatmaps depicting the ratio (fold change) of modifications in the knockout *versus* control were created by using Java Treeview.[50] Computational analysis of ETD based Middle Down proteomic data was accomplished using a mixed integer linear optimization framework as previously described.[40]

Microarray gene expression: DNA hybridization, preprocessing and analysis

RNA was extracted from control HEK293 cells and HEK293 cells that were reduced of G9a/Glp1 by siRNA for 72 h with Trizol® (Sigma), following the manufacturer's instructions. The concentration and quality of each RNA sample were assessed by nano-drop spectrophotometry and agarose gel electrophoresis. For each sample, control cells and G9a/Glp1 knockdown cells, 400 ng RNA was linearly amplified and labeled with Cy3-CTP and Cy5-CTP, respectively, using Low RNA Input Linear Amplification reagents (Agilent Technologies, Santa Clara, CA, USA). The amplified RNA was purified on RNAeasy™ spin columns (Qiagen, Valencia, CA, USA). Equal quantities (specific activity) of the amplified/labeled cRNAs from the control and G9a/Glp1 knockdown cells were mixed and competitively hybridized to Agilent 44K DNA microarrays for 17 h at 60 °C using the Agilent hybridization kit. Slides were washed according to manufacturer's protocol and scanned using an Agilent two color scanner. Raw image data were extracted using Agilent Feature extraction software and raw channel intensities were adjusted for background with a spatial de-trend algorithm. Dye normalization was performed using an intensity-dependent lowness normalization based on spots that passed a rank consistency filter, and final spot values were computed as the $\log_2$ of processed Cy3/Cy5 intensity ratios. Extracted data were then loaded onto the Princeton University PUMA database [http://puma.princeton.edu].

Spots were considered good data if intensity was well above background and the feature was not a non-uniformity outlier. Probes with duplicate measurements were averaged. Further analysis was performed in R using the Limma (Linear Models for Microarray Analysis) R software package (Limma version 2.9.1).[51] For assessing differential expression, Limma uses linear models in combination with an empirical Bayes method to moderate the standard errors of the estimated log-fold changes. The nominal *p*-values were corrected for multiple testing by false discovery rates (FDR) using the Benjamini and Hochberg approach,[52] and adjusted *p*-values <0.01 were considered significant. The set of 37 365 transcripts analyzed was used as a background for GO term enrichment. Fisher's exact test was used to test for enrichment using FuncAssociate and *p*-values were corrected using a resampling based method.[53]

Acknowledgements

References

1 P. Cheung, C. D. Allis and P. Sassone-Corsi, *Cell (Cambridge, Mass.)*, 2000, **103**, 263–271.
2 T. Jenuwein and C. D. Allis, *Science*, 2001, **293**, 1074–1080.
3 W. L. Cheung, K. Ajiro, K. Samejima, M. Kloc, P. Cheung, C. A. Mizzen, A. Beeser, L. D. Etkin, J. Chernoff, W. C. Earnshaw and C. D. Allis, *Cell (Cambridge, Mass.)*, 2003, **113**, 507–517.
4 E. Meshorer and T. Misteli, *Nat. Rev. Mol. Cell Biol.*, 2006, **7**, 540–546.
5 M. F. Fraga, E. Ballestar, A. Villar-Garea, M. Boix-Chornet, J. Espada, G. Schotta, T. Bonaldi, C. Haydon, S. Ropero, K. Petrie, N. G. Iyer, A. Perez-Rosado, E. Calvo, J. A. Lopez, A. Cano, M. J. Calasanz, D. Colomer, M. A. Piris, N. Ahn, A. Imhof, C. Caldas, T. Jenuwein and M. Esteller, *Nat. Genet.*, 2005, **37**, 391–400.
6 T. Kouzarides, *Cell (Cambridge, Mass.)*, 2007, **128**, 693–705.
7 A. J. Ruthenshaw, H. Li, D. J. Patel and C. D. Allis, *Nat. Rev. Mol. Cell Biol.*, 2007, **8**, 983–994.

8 B. E. Bernstein, A. Meissner and E. S. Lander, *Cell (Cambridge, Mass.)*, 2007, **128**, 669–681.

9 C. Bonisch, S. M. Nieratschker, N. K. Orfanos and S. B. Hake, *Expert Rev. Proteomics*, 2008, **5**, 105–119.

10 S. I. Grewal and S. Jia, *Nat. Rev. Genet.*, 2007, **8**, 35–46.

11 Y. Shi and J. R. Whetstine, *Mol. Cell*, 2007, **25**, 1–14.

12 S. Kubicek, R. J. O'Sullivan, E. M. August, E. R. Hickey, Q. Zhang, M. L. Teodoro, S. Rea, K. Mechtler, J. A. Kowalski, C. A. Homon, T. A. Kelly and T. Jenuwein, *Mol. Cell*, 2007, **25**, 473–481.

13 S. Epsztejn-Litman, N. Feldman, M. Abu-Remaileh, Y. Shufaro, A. Gerson, J. Ueda, R. Deplus, F. Fuks, Y. Shinkai, H. Cedar and Y. Bergman, *Nat. Struct. Mol. Biol.*, 2008, **15**, 1176–1183.

14 K. B. Dong, I. A. Maksakova, F. Mohn, D. Leung, R. Appanah, S. Lee, H. W. Yang, L. L. Lam, D. L. Mager, D. Schubeler, M. Tachibana, Y. Shinkai and M. C. Lorincz, *EMBO J.*, 2008, **27**, 2691–2701.

15 M. Tachibana, Y. Matsumura, M. Fukuda, H. Kimura and Y. Shinkai, *EMBO J.*, 2008, **27**, 2681–2690.

16 B. A. Garcia, J. Shabanowitz and D. F. Hunt, *Curr. Opin. Chem. Biol.*, 2007, **11**, 66–73.

17 B. A. Garcia, J. J. Pesavento, C. A. Mizzen and N. L. Kelleher, *Nat. Methods*, 2007, **4**, 487–489.

18 M. Stabell, R. Eskeland, M. Bjørkmo, J. Larsson, R. B. Aalen, A. Imhof and A. Lambertsson, *Nucleic Acids Res.*, 2006, **34**, 4609–4621.

19 M. Tachibana, K. Sugimoto, T. Fukushima and Y. Shinkai, *J. Biol. Chem.*, 2001, **276**, 25309–25317.

20 X. Zhang, Q. K. Jin, S. A. Carr and R. S. Annan, *Rapid Commun. Mass Spectrom.*, 2002, **16**, 2325–2332.

21 M. D. Plazas-Mayorca, B. M. Zee, N. L. Young, I. M. Fingerman, G. LeRoy, S. D. Briggs and B. A. Garcia, *J. Proteome Res.*, 2009, **8**, 5367–5374.

22 S. B. Hake, B. A. Garcia, E. M. Duncan, M. Kauer, G. Dellaire, J. Shabanowitz, D. P. Bazett-Jones, C. D. Allis and D. F. Hunt, *J. Biol. Chem.*, 2006, **281**, 559–568.

23 S. B. Hake and C. D. Allis, *Proc. Natl. Acad. Sci. U. S. A.*, 2006, **103**, 6428–6435.

24 Q. Feng, H. Wang, H. H. Ng, H. Erdjument-Bromage, P. Tempst, K. Struhl and Y. Zhang, *Curr. Biol.*, 2002, **12**, 1052–1058.

25 H. H. Ng, D. N. Ciccone, K. B. Morshead, M. A. Oettinger and K. Struhl, *Proc. Natl. Acad. Sci. U. S. A.*, 2003, **100**, 1820–1825.

26 C. L. Peterson and M. A. Laniel, *Curr. Biol.*, 2004, **14**, R546–R551.

27 E. McKittrick, P. R. Gafken, K. Ahmad and S. Henikoff, *Proc. Natl. Acad. Sci. U. S. A.*, 2004, **101**, 1525–1530.

28 C. Beisel, A. Imhof, J. Greene, E. Kremmer and F. Sauer, *Nature*, 2002, **419**, 857–862.

29 M. Tachibana, K. Sugimoto, M. Nozaki, J. Ueda, T. Ohta, M. Ohki, M. Fukuda, N. Takeda, H. Niida, H. Kato and Y. Shinkai, *Genes Dev.*, 2002, **16**, 1779–1791.

30 H. Tagami, D. Ray-Gallet, G. Almouzni and Y. Nakatani, *Cell (Cambridge, Mass.)*, 2004, **116**, 51–61.

31 J. J. Pesavento, C. A. Mizzen and N. L. Kelleher, *Anal. Chem.*, 2006, **78**, 4271–4280.

32 T. Hirota, J. J. Lipp, B. H. Toh and J. M. Peters, *Nature*, 2005, **438**, 1176–1180.

33 T. Suganuma and J. L. Workman, *Cell (Cambridge, Mass.)*, 2008, **135**, 604–607.

34 T. Hung, O. Binda, K. S. Champagne, A. J. Kuo, K. Johnson, H. Y. Chang, M. D. Simon, T. G. Kutateladze and O. Gozani, *Mol. Cell*, 2009, **33**, 248–256.

35 L. Jiang, J. N. Smith, S. L. Anderson, P. Ma, C. A. Mizzen and N. L. Kelleher, *J. Biol. Chem.*, 2007, **282**, 27923–27934.

36 Z. Wang, C. Zang, J. A. Rosenfeld, D. E. Schones, A. Barski, S. Cuddapah, K. Cui, T. Y. Roh, W. Peng, M. Q. Zhang and K. Zhao, *Nat. Genet.*, 2008, **40**, 897–903.

37 W. Fischle, B. S. Tseng, H. L. Dormann, B. M. Ueberheide, B. A. Garcia, J. Shabanowitz, D. F. Hunt, H. Funabiki and C. D. Allis, *Nature*, 2005, **438**, 1116–1122.

38 W. Fischle, Y. Wang and C. D. Allis, *Nature*, 2003, **425**, 475–479.

39 N. L. Young, P. A. DiMaggio, M. D. Plazas-Mayorca, R. C. Baliban, C. A. Floudas and B. A. Garcia, *Mol. Cell. Proteomics*, 2009, **8**, 2266–2284.

40 P. A. DiMaggio, N. L. Young, R. C. Baliban, B. A. Garcia and C. A. Floudas, *Mol. Cell. Proteomics*, 2009, **8**, 2527–2543.

41 J. A. Latham and S. Y. Dent, *Nat. Struct. Mol. Biol.*, 2007, **14**, 1017–1024.

42 H. N. Du, I. M. Fingerman and S. D. Briggs, *Genes Dev.*, 2008, **22**, 2786–2798.

43 D. W. Kim and A. B. Lassar, *Mol. Cell. Biol.*, 2003, **23**, 8704–8717.

44 Z. Liu, S. Zhou, L. Liao, X. Chen, M. Meistrich and J. Xu, *J. Biol. Chem.*, 2010, **285**, 2758–2270.

45 B. A. Garcia, S. A. Busby, J. Shabanowitz, D. F. Hunt and N. Mishra, *J. Proteome Res.*, 2005, **4**, 2032–2042.

46 B. A. Garcia, S. Mollah, B. M. Ueberheide, S. A. Busby, T. L. Muratore, J. Shabanowitz and D. F. Hunt, *Nat. Protoc.*, 2007, **2**, 933–938.

47 J. Rappsilber, Y. Ishihama and M. Mann, *Anal. Chem.*, 2003, **75**, 663–670.

48 D. L. Swaney, G. C. McAlister and J. J. Coon, *Nat. Methods*, 2008, **5**, 959–964.

49 M. J. MacCoss, C. C. Wu and J. R. Yates, 3rd, *Anal. Chem.*, 2002, **74**, 5593–5599.

50 A. J. Saldanha, *Bioinformatics*, 2004, **20**, 3246–3248.

51 G. K. Smyth, *Stat. Appl. Genet. Mol. Biol.*, 2004, **3**, No. 1, Article 3 (Online, Tech Report PDF).

52 Y. Benjamini and Y. Hochberg, *J. R. Stat. Soc. Ser. B (Methodological)*, 1995, **57**, 289–300.

53 G. F. Berriz, J. E. Beaver, C. Cenik, M. Tasan and F. P. Roth, *Bioinformatics*, 2009, **25**, 3043–3044.